Synthesis of Zinc Oxide nanoparticles at different aging time for low cost Dye Sensitized Solar Cells

H. A. Zayed[1], H. Musleh[1,2] S. Shaat[3], A. Issa[4], N. Shurrab[5], J. Asaad[1], N. AlDahoudi[1]

[1] Physics Department, Women`s College for Art, Science, and Education, Ain Shams University, Cairo, Egypt.

[2] Physics Department, Al Azhar University-Gaza, P.O. Box 1277, Gaza, Palestine

[3] Physics Department, Islamic University of Gaza, P.O. Box 108, Gaza, Palestine

[4] Engineering Department, Al Azhar University-Gaza, P.O. Box 1277, Gaza, Palestine

[5] Chemistry Department, Al Azhar University-Gaza, P.O. Box 1277, Gaza, Palestine

Abstract

Zinc oxide nanoparticles synthesized via simple precipitation method and aged at different time were used as photoanodes of dye sensitized solar cells (DSSCs). The structural and the optical properties of the obtained zinc oxide nanoparticles were investigated. The performance of the assembled solar cells was studied and the efficiency of such cell was compared as a relation of the aging time of the ZnO nanoparticles.

Key words

Zinc oxide, nanoparticles, precipitation method, dye sensitized solar cell

Introduction

The wide band gap semiconductor of band gap > 3.2eV , with a high exciton binding energy of 60 meV and its high electron mobility make Zinc oxide as one of the most interested candidates for many technological multidisciplinary applications, such as in solar energy conversion, thin film transistors, catalysis, nonlinear optics, gas sensors, pigments, cosmetic, etc. (Chou, et al. 2007; Gao and Wang 2005; Hachigo, et al. 1994; Han and Kim 1998; Harada, et al. 1992; Hotchandani and Kamat 1992; Ko, et al. 2003; Lee, et al. 1995; Lieri, et al. 2005; Morkoc, et al. 1994; Sakohara, et al. 1992; Shishiyanu, et al. 2005). Nanostructured size zinc oxide can be found in different forms, like nanoparticles, nanorods, nanobelt, nanoflowers, etc.(Kharisov 2008; Li, et al. 2011; Liu, et al. 2004; Yi, et al. 2005; Yum, et al. 2008). It is favorable for electron transport, easily crystallized and anisotropically grow in a variety of morphologies. Due to its unique properties, it has been proposed as alternative photoelectrodes in Dye Sensitized Solar Cells (DSSCs) in order to achieve better performance.

DSSCs have attracted much attention due to their low cost manufacturing, fabrication on flexible substrate and simple construction (Grätzel 2003; Hagfeldt, et al. 2010). Despite these advantages, the maximum certified efficiency for DSSCs is much lower compared to silicon based solar cells. Much research has been focused to enhance the performance of

DSSCs with different anode materials. Common photoanode materials in DSSCs are TiO_2, ZnO NPs film on transparent conducting oxide (TCO) layers (Grätzel 2003). The popularity of such materials is due to their large surface area and chemical affinity for dye adsorption as well as their suitable energy band potential for charge transfer with dye and electrolytes (Grätzel 1991)(Bandara, et al. 2005). The structure and morphology of the photoelectrode play a vital role in developing such materials (Kuang, et al. 2007). The improvement of the conversion efficiency can be attributed to the larger surface area, which is a goal of most researchers.

In this work, zinc oxide nanoparticles were synthesized using simple precipitation method and aged at different periods. The structural and optical properties of the obtained nanoparticles were characterized using different techniques. Solar cells were assembled using the different synthesized nanoparticles as photoanode. Their performance parameters were investigated and a comparative study was presented.

Experimental Set Up

Synthesis of the ZnO nanoparticles

ZnO NPs were synthesized using simple precipitation method at different aging time. 8.0 g of $Zn(CH_3COO)_2 2H_2O$ (*Zn Ac*) was dissolved into 100 ml of pure methanol under vigorous stirring for 30 min at 60℃ followed by sonication for 30 min until a clear and transparence solution was obtained. Dissolving of $Zn\,Ac$ into hot methanol completely under vigorous storing means total hydrolysis of $Zn\,Ac$ forming acetate ions and Zn ions. 5M $NaOH$ solution was added drop wise into the acetate solution under vigorous stirring until the pH reached 12. Then, the clear solution was transferred to milky white slurry suspension. The white precipitate was stirred for different aging times of 20, 30, 60 and 90 min that were titled as S1, S2, S3 and S4, respectively. After that, the precipitate was stirred slowly at room temperature overnight. White precipitates were carefully collected and washed with absolute ethanol five times for 1.5 hours using centrifugation at $3500\ rpm$ to remove the non reacted materials. Zinc hydroxide can be, easily, converted to $ZnO\ NPs$ by drying. So, the product dried at 65℃ overnight. Finally, the product crashed using mortar and pestle to produce fine powder. The structural properties of the $ZnO\ NPs$ were characterized using different techniques.

The structural characterization of the obtained nanoparticles was carried out using an X-ray diffractometer (XRD) (type: Philips Expert), using Cu anode material operating at 40 kV and 30 mA with ($\lambda = 1.5418\ A^o$) employing a scanning rate of $0.02^o s^{-1}$.

Transmission electron microscopy (TEM) is a good tool to determine the particle size and morphology of the nanoparticles down to a nanometer scale as well their crystalline structure. Their structure were characterized using a high resolution transmission electron microscopy ($type$: $(JEM - 2100), JEOL$).

The $UV - VIS$ absorption measurements have been performed using double beam $Shimadzu\ UV - 1601\ PC$ with a diffraction gritting with self-aligning, energy- optimizing deuterium lamp for ultraviolet region and halogen lamp for visible region to enhance the accuracy across the $UV - VIS$ spectrum and into the near infrared (NIR).

Fabricate and assembly the device (Solar cell)

The pastes of$ZnO\ NPs$were prepared by mixing 0.3 g of ZnO nanopowder with 0.6 g of Polyethylene glycol ($PEG400$) using a mortar and pestle for 10 minutes. The pastes were deposited on fluorine-doped SnO_2(FTO) coated glass substrates, using the ‘‘doctor blade’’ technique forming 0.5 × 0.5 cm layers. The layers were dried at 100°C for 60 min followed by sintering them at 450°C for 1 h in air. The obtained sintered layers had a thickness between 12 to 15 μm. The prepared layers of ZnO photoanode were immersed to sensitize them in $0.32\ mMEosin\ B$ for 24 h. After that films were rinsed in ethanol and were dried in air at room temperature. A Pt-coated FTO substrate was used as the counter electrode and an iodide-based solution, consisting of $0.6M\ tetra - butylammonium\ iodide$, $0.1M\ lithium\ iodide$, $0.1M\ iodine$ and $0.5M\ 4 - tert - butylpyridine$ in $acetonitrile$ was used as the liquid electrolyte.

Photovoltaic properties of $DSSCs$ were characterized using simulated AM 1.5 sunlight illumination with an output power of $100\ mW/cm^2$.

Results & Discussions

X-ray diffraction (XRD) patterns was used to provide the information about the crystal structure and the grain size of the NPs. Fig. 1 depicts the XRD patterns of the of thesamples S1, S2, S3 and S4 of the synthesized $ZnO\ NPs$. The XRD patterns of the synthesized samples matched with the standard hexagonal wurtzite structure phase of ZnO ($ICSD\ card\ No.\ 067454$). Fig. 1 indicates that the XRD patterns have gradual sharpness

of the peaks as the aging time increases, which means that the particle size increases gradually. No other phases have been observed, which further confirmed the formation of pure $ZnO\ NPs$ with single phase. The sharpness of the broaden XRD diffraction peaks are indicated to the small size and the good crystallinity of the NPs. Different lattice parameters were calculated from XRD patterns of the $ZnO\ NPs$ and tabulated in table 1, which was agreed with the results were reported in ref. (Thomas 2014). The average particle size (D) of the NPs were estimated from the broadening of the highest intensity peak (101) by Debye-Scherrer's formula, which showed increasing from 18.70 to 26.83 nm with increasing of the aging time from 20 to 90 min. as shown in table 1. The dislocation density ($\delta = 1/D^2$), which represents the amount of defects in the sample is defined as the length of dislocation lines per unit volume (V) of the crystal and irregularity within a crystal structure. (Thomas 2014). The calculated values of δ decreased from 2.86 to 1.50 nm^{-2} with the increasing of the particle size and the aging time as depicted in Table 1. The strain ($\varepsilon = \beta/4\tan(\theta)$) where β is the full width at half maximum), which can be defined by the change in size to the original size of the particle (Ahmad Monsh 2012). The obtained values of ε decreased from 10.3×10^{-4} to 7.46×10^{-4}as the particle size increased with increases of the aging time.

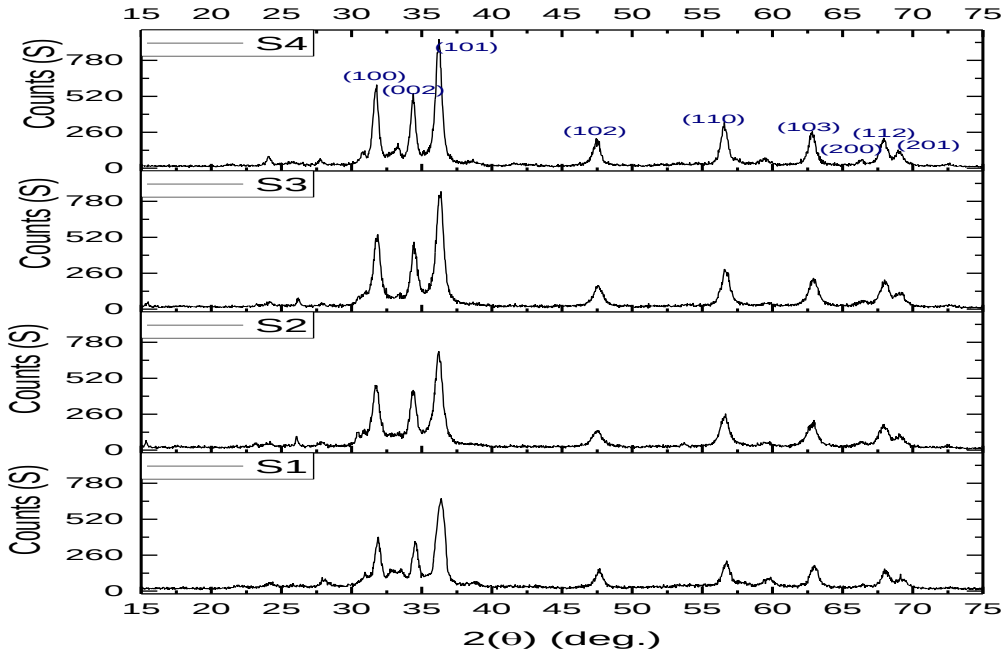

Fig. 1: XRD patterns of the samples S1, S2, S3 and S4 of the synthesized ZnO NPs

Table 1: XRD calculated Geometric parameters of the samples S1, S2, S3 and S4 of the synthesized ZnO NPs.

#	a (nm)	c (nm)	(c/a)	V (nm^3)	β $(deg.)$	D (nm)	$\delta * 10^{-3}$ (nm^{-2})	$\varepsilon * 10^{-4}$
S1	**3.2405**	**5.1663**	**1.5943**	**46.981 6**	**0.742**	**18.700**	**2.86**	**10.3**
S2	**3.2373**	**5.21 3**	**1.6102**	**47.31 20**	**0.7109**	**19.504**	**2.63**	**9.85**
S3	**3.2435**	**5.2249**	**1.6109**	**47.602**	**0.52**	**25.781**	**1.50**	**7.16**
S4	**3.241**	**5.293**	**1.633**	**48.150 7**	**0.500**	**26.830**	**1.50**	**7.46**

High Resolution Transmission Electron Microscopy (HRTEM)

The morphology of the sample S3 of the synthesized $ZnO\ NPs$ was studied by high-resolution transmission electron microscopy ($HRTEM$).

Fig. 2(a) depicts the high-resolution image of sample S3 of $ZnO\ NPs$and the sharp boundary of the spherical particle can be seen. Fig. 2 (b)shows the diffraction patterns.Theselected electron diffraction area ($SAED$) pattern and the histogram of the sample S3 of the synthesized $ZnO\ NPs$ are shown in Figs. 2(c and d). As shown in Fig. 2(a) $ZnO\ NPs$ was crystalline, spherical and uniform with average particle size 23 nm which is very closed to the estimated averaged particle size of range of 18.7 to 26.8 nm from the XRD pattern broadening. The spacing between the adjacent lattice planes distance (d) of the sample S3 of the synthesized $ZnO\ NPs$ was measured from the bright field $SAED$ patterns, which was founded to be 0.2457. The obtained value of d of 0.2457 nm is in good agreement with the obtained value from XRD results, which corresponds to the (102) plane of ZnO.

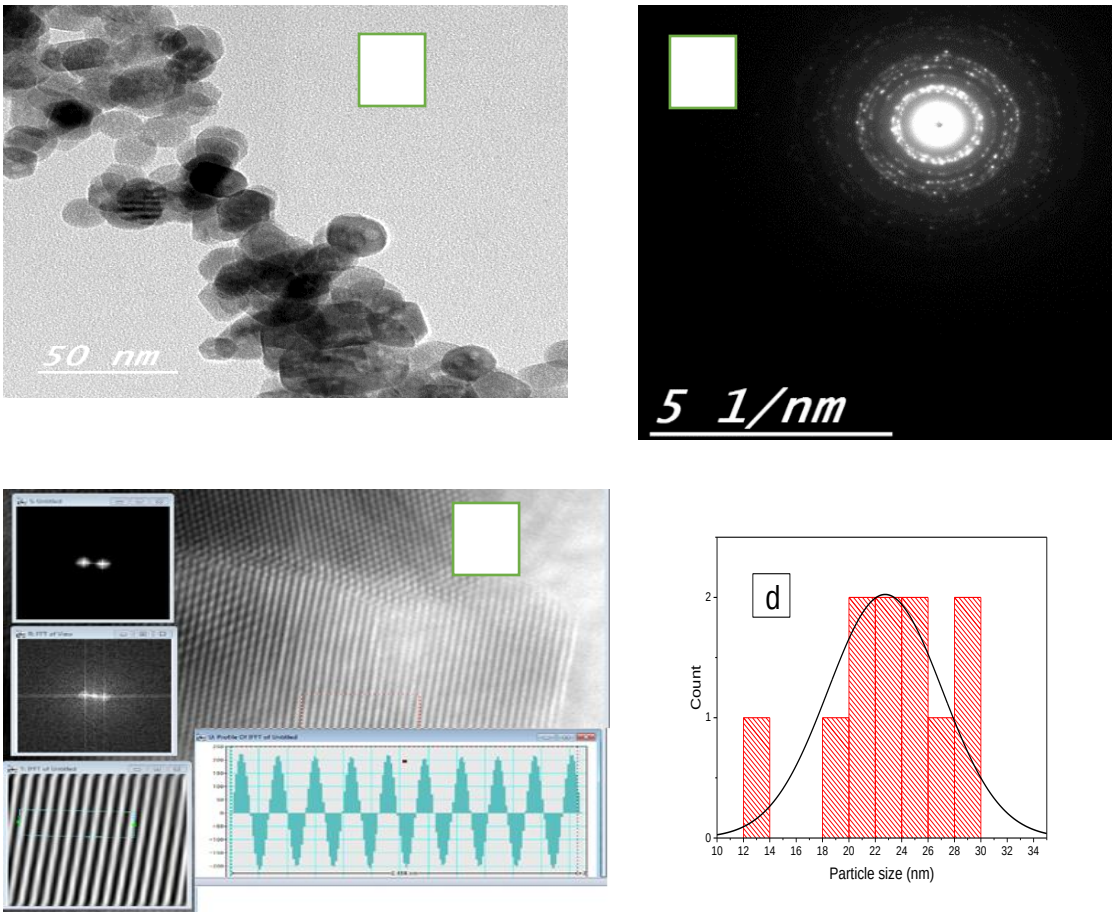

Fig. 2 HRTEM micrograph of (S3) ZnO nanoparticles sample (a) micrograph image, (b) Diffraction patterns and (c) selected electron diffraction area and (d) histograms

UV-VIS absorption characterization

The effect of the aging time on the optical properties of synthesized of$ZnO\ NPs$ were studied by $UV-VIS$ absorption spectroscopy. Fig. (3) represents the typical$UV-VIS$ absorption spectra of the samples S1, S2, S3 and S4 of the synthesized ZnO NPs, which are recorded at room temperature. This figure indicates that, the corresponding absorption edge was positioned at 353, 364, 365 and 368 nm for the samples S1, S2, S3 and S4, respectively. These peaks indicates that the absorption edges shifted towards the higher value of wavelength (red shift) with increasing of the aging time. This shift may be attributed to the increasing of the average particle size, which agrees with the study in ref. (Almoqayyad 2012). Based on the $UV-VIS$ absorption spectroscopy of the samples S1, S2, S3 and S4 of the synthesized $ZnO\ NPs$. The energy gap (E_g) was estimated using Tauc Davis and Mott relation $(\alpha hv)^2 \propto (hv - E_g)$, as shown in Fig. (4). The estimated values of Eg were decreased from 3.52 eV to 3.36 eV as increases of the aging time from 20 to 90 min. This shift may attributed to the increasing of the average particle size, which agrees with studies by (Almoqayyad 2012).

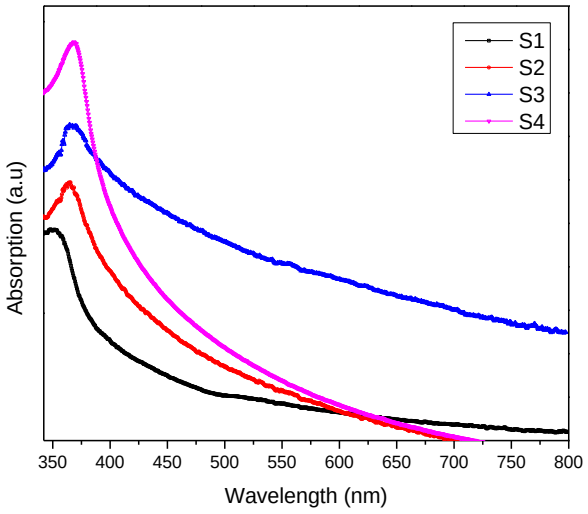

Fig. (3) UV-VIS. spectra of pure ZnO nanoparticle samples S1, S2, S3 and S4 at different aging times using simple precipitation method.

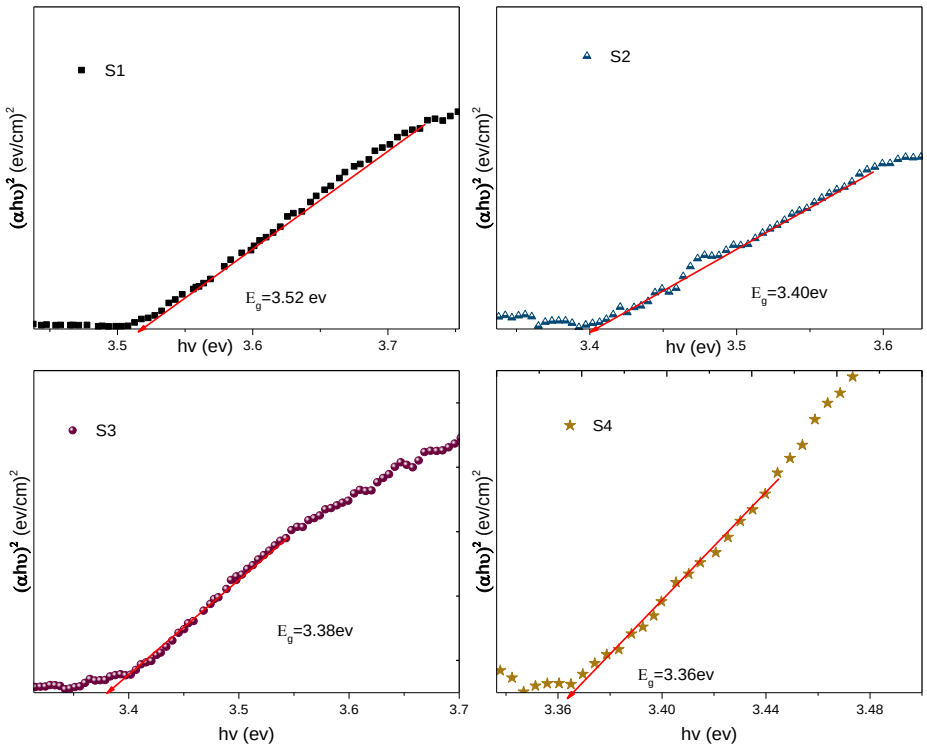

Fig. (4)$(\alpha h\nu)^2$versus the photon energy $(h\nu)$of pure ZnO nanoparticles S1, S2, S3 and S4 at different aging times using simple precipitation method.

Cell Performance

The performance of the synthesized ZnO as a semiconducting photoanode layer was tested using $EosinB$ as dye sensitizer. The characteristics $J-V$ curves of different DSSCs fabricated with different nanoparticles that aged at different times S1 to S4 are depicted in Fig. (5). For each cell, the measured current density versus the applied voltage V is obtained at the incident light intensity of 100 $mWm^{-2.}$ The resulted power is plotted versus the applied voltage as shown in Fig. (6). This study shows the benefits of increasing the aging time. The performace parameters of the measurements are summarized in table 2. It is shown that the cell S3 exhibited the highest efficiency and the best performance parameters were obtained. It has an open circuit voltage, V_{oc} = 0.374 V, a photocurrent density J_{sc} =0.890 $mAcm^{-2}$,maximum power P_m = 0.204 $mWcm^{-2}$, filling factor FF = 61.7 %, and an overall photo to electric conversion efficiency η = 0.205 %. The open circuit voltage ranges between 0.34 V for the cell S2 and 0.454 V for S1, while

the current density has the maximum value of 0.985 for the cell S1, and the minimum value of 0.577 for the cell S4. The increase of the open circuit may be attributed to less charge recombination, and the increase of the charge injection results to an increase of the photocurrent density. This may be attributed to more dye loading on the surface of the nanoparticles. The fill factor of the fabricated cells ranges from 49% to 61.7% for S1 and S3, respectively. The highest fill factor was observed for the S3 and the lowest fill factor was obtained for the cell S2.

In general the cell S1and the cell S3, have relatively higher value of the output power and efficiency, on the other hand the cell S2and the cell S4, have relatively lower value of the output power and efficiency. Generally, the low values of current density may be attributed to missing of the anchoring group in the chemical structure of $Eosin\ B$. Ideal sensitizer must have at least one anchoring group such as, $-PO_3H_2$, $-\mathrm{Py}$, $-\mathrm{COOH}$ and,$-\mathrm{SO_3H}$. This groups makes a strong link between ZnO semiconductor surface and the dye molecule, in order to enhance electron injection from the $LUMO$ energy level of the dye molecule to the conduction band of the semiconductor layer (Calogero, et al. 2015).

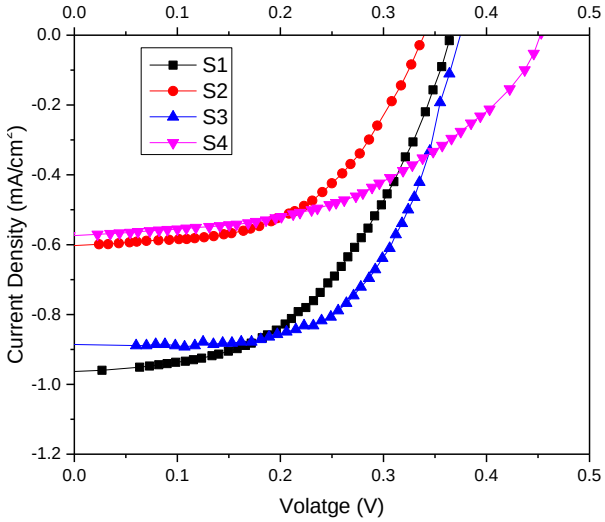

Fig. (5) J-V curves of pure ZnO nanoparticle samples S1, S2, S3 and S4 aged at different aging times using simple precipitation method.

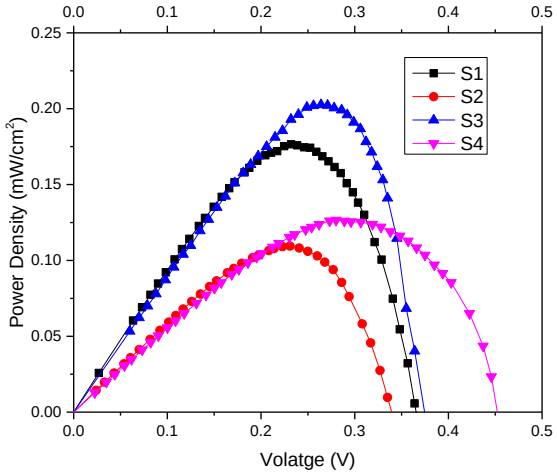

Fig. (6) P-V curves of pure ZnO nanoparticle samples S1, S2, S3 and S4 at different aging times using simple precipitation method.

Table2: Photovoltaic parameters of the DSSCs fabricated using pure ZnO NPs samples S1, S2, S3 and S4 using simple precipitation method.

	J_{sc} (mA/cm^2)	V_{oc} (V)	J_m (mA/cm^2)	V_m (mV)	P_m (mW/cm^2)	FF %	η %
S1	0.964	0.365	0.763	0.232	0.177	50.30	0.177
S2	0.61	0.34	0.474	0.232	0.11	35.02	0.110
S3	0.890	0.374	0.768	0.267	0.204	61.70	0.205
S4	0.577	0.454	0.452	0.278	0.127	48.00	0.126

Conclusion

It was concluded that the aging time of the zinc oxide nanoparticles influences their structural properties. An increase of the particle size was calculated by increasing the aging time, which is in agreement of the shift found in their absorption spectrum. The performance of the solar cells, i.e. the short circuit photocurrent density and the open circuit voltage was affected by the aging time of the obtained nanoparticles. The best photo to electric conversion efficiency for the cell based on the zinc oxide nanoparticles

sample (S3) that aged for 60 minutes was the optimum using the low cost $Eosin\ B$ dye with efficiency of 0.205%.

Acknowledgement

The research activities in Gaza were financially supported by Qatar Charity IBHATH Project grant funded by the Gulf Cooperation Council for the Reconstruction of Gaza through the Islamic Development Bank.

References

Ahmad Monsh, Mohammad Reza Forough, Mohammad Reza Monshi, 2012 Modified Scherrer Equation to Estimate More Accurately Nano-Crystallite Size Using XRD,World Journal of Nano Science and Engineering 2:154-160.

Almoqayyad, Sami Ibrahim, 2012 Study of Synthesis and Growth of ZnO Nanoparticles Chemistry department, Al-Azhar University of Gaza. M.Sc.Thesies.

Bandara, J, UW Pradeep, and RGSJ Bandara, 2005 The role of n–p junction electrodes in minimizing the charge recombination and enhancement of photocurrent and photovoltage in dye sensitized solar cells. Journal of Photochemistry and Photobiology A: Chemistry 170(3):273-278.

Calogero, G., et al. 2015 Vegetable-based dye-sensitized solar cells. Chem Soc Rev 44(10):3244-94.

Chou, Tammy P, et al. 2007 Hierarchically Structured ZnO Film for Dye- Sensitized Solar Cells with Enhanced Energy Conversion Efficiency. Advanced Materials 19(18):2588-2592.

Gao, Pu Xian, and Zhong L Wang 2005 Nanoarchitectures of semiconducting and piezoelectric zinc oxide. Journal of Applied physics 97(4):044304.

Grätzel, B. O'Regan and M. 1991 A low cost high-efficiency solar cell based on dyesensitized colloidal TiO2 films. Nature 353:737-740

Grätzel, Michael, 2003 Dye-sensitized solar cells. Journal of Photochemistry and Photobiology C: Photochemistry Reviews 4(2):145-153.

Hachigo, Akihiro, et al. 1994 Heteroepitaxial growth of ZnO films on diamond (111) plane by magnetron sputtering. Applied physics letters 65(20):2556-2558.

Hagfeldt, Anders, et al. 2010 Dye-sensitized solar cells. Chemical reviews 110(11):6595-6663.

Han, Joo-Hwan, and Doh-Yeon Kim,1998 Fabrication of dense Zno-varistors by atmosphere sintering. Journal of the European Ceramic Society 18(7):765-770.

Harada, Masafumi, et al. 1992 Structure of polymer-protected palladium-platinum bimetallic clusters at the oxidized state: extended x-ray absorption fine structure analysis. The Journal of Physical Chemistry 96(24):9730-9738.

Hotchandani, Surat, and Prashant V Kamat, 1992 Photoelectrochemistry of semiconductor ZnO particulate films. Journal of the Electrochemical Society 139(6):1630-1634.

Kharisov, Boris I, 2008 A review for synthesis of nanoflowers. Recent patents on nanotechnology 2(3):190-200.

Ko, Sang Choon, et al. 2003 Micromachined piezoelectric membrane acoustic device. Sensors and Actuators A: Physical 103(1):130-134.

Kuang, Daibin, et al. 2007 High- Efficiency and Stable Mesoscopic Dye- Sensitized Solar Cells Based on a High Molar Extinction Coefficient Ruthenium Sensitizer and Nonvolatile Electrolyte. Advanced Materials 19(8):1133-1137.

Lee, J, et al. 1995 Impedance spectroscopy of grain boundaries in nanophase ZnO. Journal of materials research 10(09):2295-2300.

Li, Liang, et al. 2011 High-yield synthesis of single-crystalline zinc oxide nanobelts and their applications in novel Schottky solar cells. Chemical Communications 47(29):8247-8249.

Lieri, GS, et al. 2005 A novel method for the preparation of NH 3 sensors based on ZnO-In thin films. Sens Actuators B 25:588-590.

Liu, Xiang, et al. 2004 Growth mechanism and properties of ZnO nanorods synthesized by plasma-enhanced chemical vapor deposition. Journal of Applied Physics 95(6):3141-3147.

Morkoc, H, et al. 1994 Large- band- gap SiC, III- V nitride, and II- VI ZnSe- based semiconductor device technologies. Journal of Applied Physics 76(3):1363-1398.

Sakohara, Shuji, Lane D Tickanen, and Marc A Anderson , 1992 Luminescence properties of thin zinc oxide membranes prepared by the sol-gel technique: change in visible luminescence during firing. The Journal of Physical Chemistry 96(26):11086-11091.

Shishiyanu, Sergiu T, Teodor S Shishiyanu, and Oleg I Lupan, 2005 Sensing characteristics of tin-doped ZnO thin films as NO 2 gas sensor. Sensors and Actuators B: Chemical 107(1):379-386.

Thomas, P. Bindu • Sabu 2014 Estimation of lattice strain in ZnO nanoparticles: X-ray peak profile analysis. J Theor Appl Phys 8::123–134.

Yi, Gyu-Chul, Chunrui Wang, and Won Il Park 2005 ZnO nanorods: synthesis, characterization and applications. Semiconductor Science and Technology 20(4):S22.

Yum, J. H., et al. 2008 Recent Developments in Solid-State Dye-Sensitized Solar Cells. CHEM SUS CHEM 1(8/9):699-707.

تخليق جسيمات نانوية من أكسيد الزنك عند أزمنة تسخين مختلفة باستخدام طريقة الترسيب البسيطة

أ.د. حمدية عبد الحميد زايد[1]، حسام مصلح[1,2]، د. سامي شعث[3] ، د. أحمد عيسي[4]،
د. نبيل شراب[5]،جهاد أسعد[2]، أ.د. ناجي الداهودي[2]

(1) كلية البنات للاداب والعلوم والتربية - جامعة عين شمس – القاهرة - مصر
(2) جامعة الازهر- قسم الفيزياء-غزة- فلسطين
(3) الجامعة الاسلامية- قسم الفيزياء –غزة - فلسطين
(4) جامعة الازهر – قسم الهندسة –غزة – فلسطين
(5) جامعة الازهر – قسم الكيمياء – غزة - فلسطين

ملخص العربي

في هذا البحث تم تخليق جسيمات نانوية من أكسيد الزنك باستخدام طريقة الترسيب البسيطة و عند أزمنة تسخين مختلة لانتاج خلايا شمسية صبغية رخيصة الثمن. وقد تم دراسة بعض الخواص التركيبية والضوئية للعينات. وقيست منحنيات الخصائص الكهربية المميزة لكل خلية مصنعة كعلاقة بين تغير التيار مع الفولت. تم تعينن البارامتيرات الهامة لكل خلية مثل تيار القصر J_{sc} و جهد الدائرة المفتوحة V_{oc} و اعلي قدرة كهربية للخلية $P_m = V_m * J_m$ ومعامل الامتلاء FF واعلي كفاءة للخلية η.